Journal of Orthopaedic Research

Unfolding of membrane ruffles of in situ chondrocytes under compressive loads

Journal:	*Journal of Orthopaedic Research*
Manuscript ID	JOR-15-0838.R1
Wiley - Manuscript type:	Research Article (Member)
Date Submitted by the Author:	n/a
Complete List of Authors:	Moo, Eng Kuan; University of Calgary, Human Performance Laboratory Herzog, Walter; University of Calgary, Faculty of Kinesiology
Areas of Expertise:	osteoarthritis, membrane reservoir, articular cartilage, impact loading, knee joint
Keywords:	Cell and Molecular Imaging < Cartilage, Synovium & Osteoarthritis, Mechanobiology < Cartilage, Synovium & Osteoarthritis, Mechanics < Cartilage, Synovium & Osteoarthritis, Post Traumatic OA < Cartilage, Synovium & Osteoarthritis

SCHOLARONE™
Manuscripts

Title page

Title:

Unfolding of membrane ruffles of in situ chondrocytes under compressive loads

Authors:

Eng Kuan **Moo,** Walter **Herzog**

Affiliations:

Human Performance Laboratory, Faculty of Kinesiology, University of Calgary, Calgary, Alberta, Canada

Email address:

Eng Kuan Moo – ekmoo@ucalgary.ca

Walter Herzog – wherzog@ucalgary.ca

Corresponding author:

Name: Walter Herzog

Address: Human Performance Laboratory, University of Calgary, 2500 University Drive N.W., Calgary, Alberta, T2N 1N4, Canada.

Tel: +1 403 220 8525; E-mail: wherzog@ucalgary.ca

For Peer Review

Type of manuscript:

Full length original research article

Author contribution

All authors have read and approved the final submitted manuscript. The contributions of authors (addressed in last name) are described briefly below:

Study Design: Moo, Herzog

Acquisition of Data: Moo

Analysis and Interpretation of Data: Moo, Herzog

Manuscript Preparation, Critical Revision, Final Approval: Moo, Herzog

Statistical Analysis: Moo

Word count:

3488 words (excluding figure legends)

4015 words (including figure legends)

Running title: (< 5 words)

Membrane unfolding protects chondrocytes

For Peer Review

Abstract

Impact loading results in chondrocyte death. Previous studies implicated high tensile strain rates in chondrocyte membranes as the cause of impact-induced cell deaths. However, this hypothesis relies on the untested assumption that chondrocyte membranes unfold in vivo during physiological tissue compression, but do not unfold during impact loading. Although membrane unfolding has been observed in isolated chondrocytes during osmotically induced swelling and mechanical compression, it is not known if membrane unfolding also occurs in chondrocytes embedded in their natural extracellular matrix. This study was aimed at quantifying changes in membrane morphology of in situ superficial zone chondrocytes during slow physiological cartilage compression. Bovine cartilage-bone explants were loaded at 5μm/s to nominal compressive strains ranging from 0-50%. After holding the final strains for 45min, the loaded cartilage was chemically pre-fixed for 12h. The cartilage layer was post-processed for visualization of cell ultrastructure using electron microscopy. The changes in membrane morphology in superficial zone cells were quantified from planar electron micrographs by measuring the roughness and the complexity of the cell surfaces. Qualitatively, the cell surface ruffles that existed before loading disappeared when cartilage was loaded. Quantitatively, the roughness and complexity of cell surfaces decreased with increasing load magnitudes, suggesting a load-dependent use of membrane reservoirs. Chondrocyte membranes unfold in a load-dependent manner when cartilage is compressed. Under physiologically meaningful loading conditions, the cells likely expand their surface through unfolding of the membrane ruffles and therefore avoid direct stretch of the cell membrane.

For Peer Review

Keywords:

Osteoarthritis, articular cartilage, impact loading, knee joint, cell death, membrane reservoir, fractal analysis, caveolae

For Peer Review

Introduction

Chondrocytes are the only cell type in cartilage. They actively regulate the extracellular matrix (ECM) metabolism. Chondrocytes have a slow turnover rate, therefore injury-related cell death reduces the number of active chondrocytes, which, if severe enough, triggers tissue degradation as the living cells are not sufficient to maintain tissue structure and integrity.[1-3] Therefore, chondrocyte death has been regarded as a primary trigger for the development of osteoarthritis (OA).[1]

Chondrocyte death can occur in two modes: apoptosis or necrosis.[4, 5] While apoptosis is a form of programmed cell death that takes time to happen, chondrocyte necrosis occurs immediately after an insult to cartilage, typically through a loss of integrity of the cell membrane.[4, 5] Most cell membranes exhibit a very small elastic range (3-4%) and will rupture when stretched beyond the elastic limit.[6-9] However, isolated chondrocytes have been shown to withstand up to 78% compressive strain with a corresponding local elongation of cell membranes of >25%.[10, 11] In situ chondrocytes were also found to have up to 26% increase in overall apparent surface area when the cartilage tissue was loaded by 15% nominal compressive strains.[12] Since cell membranes rupture much before they reach 25% strain, chondrocytes must have ways for membrane elongation that does not involve direct stretching of the membrane.

Cell membranes behave like two-dimensional (2D) fluids with negligible shear rigidity.[13, 14] When the cell surface area increases because of deformation or cell volume changes, the associated membrane strain is thought to be accommodated by an unfolding of the so-called

For Peer Review

surface ruffles (folds in the cell membrane) which protects cell membranes from direct stretch.[15-17] The ability of chondrocyte membranes to absorb strains through unfolding of the surface ruffles (also referred to as the membrane reservoir) has formed the basis of mechanistic models of impact-induced chondrocyte deaths.[11, 18] Impact loading is thought to cause exceedingly high membrane strain rates, which in turn is supposed to limit membrane unfolding, thus causing direct membrane stretch and rupture once the small elastic limit of the membrane is exceeded. This proposition is partly supported by experimental evidence,[18-20] and relies on the untested assumption that chondrocyte membranes unfold in vivo for physiological tissue compression rates, but do not unfold, or only unfold to a limited degree, during impact loading rates.

Although membrane unfolding has been observed in isolated chondrocytes during osmotically induced swelling[21] and mechanical compression,[22] it is not known if membrane unfolding also occurs in chondrocytes that are embedded in their natural extracellular matrix environment. Therefore, the purpose of this study was to quantify changes in membrane morphology of in situ superficial zone chondrocytes during slow physiological cartilage compression. We hypothesized that membrane unfolding occurs for these conditions, thus providing support for our proposal that membrane unfolding may play a major role in protecting chondrocytes from death by membrane rupture during physiological loading conditions.

For Peer Review

Methods

SPECIMEN PREPARATION AND MECHANICAL LOADING PROTOCOL

Metatarsal-phalangeal joints of 24 month-old cows (N_{cow} = 14) were obtained from the local abattoir. Two osteo-chondral blocks were aseptically harvested from the proximal, medial surface of the joints, and maintained in phosphate-buffered saline (P5368, Sigma-Aldrich, ON, Canada). The osteo-chondral samples were randomly assigned to either the control-unloaded group or the strain-loaded group (10% strain, $N_{explant}$ = 5; 30% strain, $N_{explant}$ = 4; 50% strain, $N_{explant}$ = 5).

Mechanical compression of cartilages was performed on the day of explant harvest. Briefly, full-thickness cartilages attached to the underlying bones were cut using a 6-mm circular punch before being attached to a specimen holder using dental cement. Tissue thickness was determined by needle indentation at four locations close to the loaded region. Hydrated cartilages were indented using a flat-ended, impermeable, cylindrical (2 mm diameter) indenter attached to a servo-hydraulic material testing system (MTS 858 Mini Bionix II, MTS Systems Corp., AB, Canada) in a stress-relaxation mode. A load cell was fitted between the indenter and the MTS system in order to record the reaction force resulting from tissue compression. The applied stress was calculated by dividing the tissue reaction force by the area of the indenter. The cartilages were compressed to nominal tissue strains of 0 %, 10 %, 30 %, and 50 % at a constant rate of 5 µm/s.

For Peer Review

After holding the load for ~45min, the saline solution was replaced by a pre-fixative solution consisting of 0.7 % ruthenium hexammine trichloride (RHT) and 2 % glutaraldehyde in 0.05 M cacodylate buffer at pH 7.4. After pre-fixing the sample for 12 h, the indenter was removed and full-thickness cartilages containing the indented area were cut from the underlying bone and kept in the pre-fixative solution overnight.

ELECTRON MICROSCOPY

Cartilage samples were immersed in 0.1M cacodylate buffer containing 1.6% paraformaldehyde, 0.7% RHT and 2.5% glutaraldehyde at pH 7.4 (2 h). After washing three times with the same buffer, the samples were post-fixed in 1% osmium tetroxide buffered with 0.1 M cacodylate buffer at pH 7.4 (2 h). Samples were then stained with 0.5 % uranyl acetate (1 h) and dehydrated through a graded series of ethanol prior to embedding in Spurr's resin. Ultrathin sections (~70 nm) were cut using a diamond knife mounted on an ultra-microtome (Ultracut E, Leica-Reichert Jung, Wetzlar, Germany) along the direction of tissue thickness prior to staining using 2% aqueous uranyl acetate and Reynolds' lead citrate.

The ultrathin sections were imaged by a transmission electron microscope (H-7650, Hitachi High Technologies America Inc., CA, USA) at an accelerating voltage of 80 kV. 2D micrographs of individual chondrocytes (N_{cell} = 22 for each of the loading groups) with well-defined nuclei in the superficial zone tissues (the top 7.5% tissue thickness) were taken at a magnification of either 6,000x (for unloaded cartilages) or 20,000x (for loaded cartilages) through a mounted AMT 16000 digital camera.

For Peer Review

IMAGE ANALYSIS

Changes in chondrocyte membrane morphology as a function of tissue compression were analyzed using measures of surface roughness and surface complexity. 2-6 individual chondrocytes were selected for analysis from each tissue explant.

In order to quantify surface roughness, the circumference of individual cells was manually-tracked to obtain the true cell circumference (red solid outline, Fig. 1). The region enclosed by the true cell circumference was then best-fit to an ellipse (green dash-dotted outline, Fig. 1) of equal area and second moment of area.[23] In addition, a best-fitting cubic spline was used to approximate the outline of cells (blue dashed outline, Figure 1). Surface roughness was defined as the percentage difference in circumference between the cell and the fitted ellipse (ellipse-fitted roughness). As there may be a mismatch between the actual cell shape and the best fitting ellipse, we also used a spline-fitting approach (spline-fitted roughness) that uses cubic spline segments to approximate the cell shapes more accurately and to assess the validity of the simpler ellipse-fitted surface roughness.

In order to measure the surface complexity, fractal analysis was performed on the membrane morphology. The manually-tracked cell circumference was analysed through the box-counting method using the plugin 'FracLac' algorithm (Karperien, A., version 2.5, url: http://rsb.info.nih.gov/ij/plugins/fraclac/FLHelp/BoxCounting.htm) in ImageJ (National Institutes of Health, MD, USA). Briefly, cell images were overlaid with a grid of known size

For Peer Review

(box size) and the number of boxes that contain the cell membrane (box count) was quantified. This process was repeated using multiple grids of decreasing sizes. The box counting fractal dimension was obtained from the slope of the linear regression line estimated from the natural logarithmic plot of box count against box size (see Supplementary Materials, S1, for more details).

The shape of cells was described by the aspect ratio, defined as the ratio of the lengths of the major to the minor axis of the best-fitting ellipse.

For Peer Review

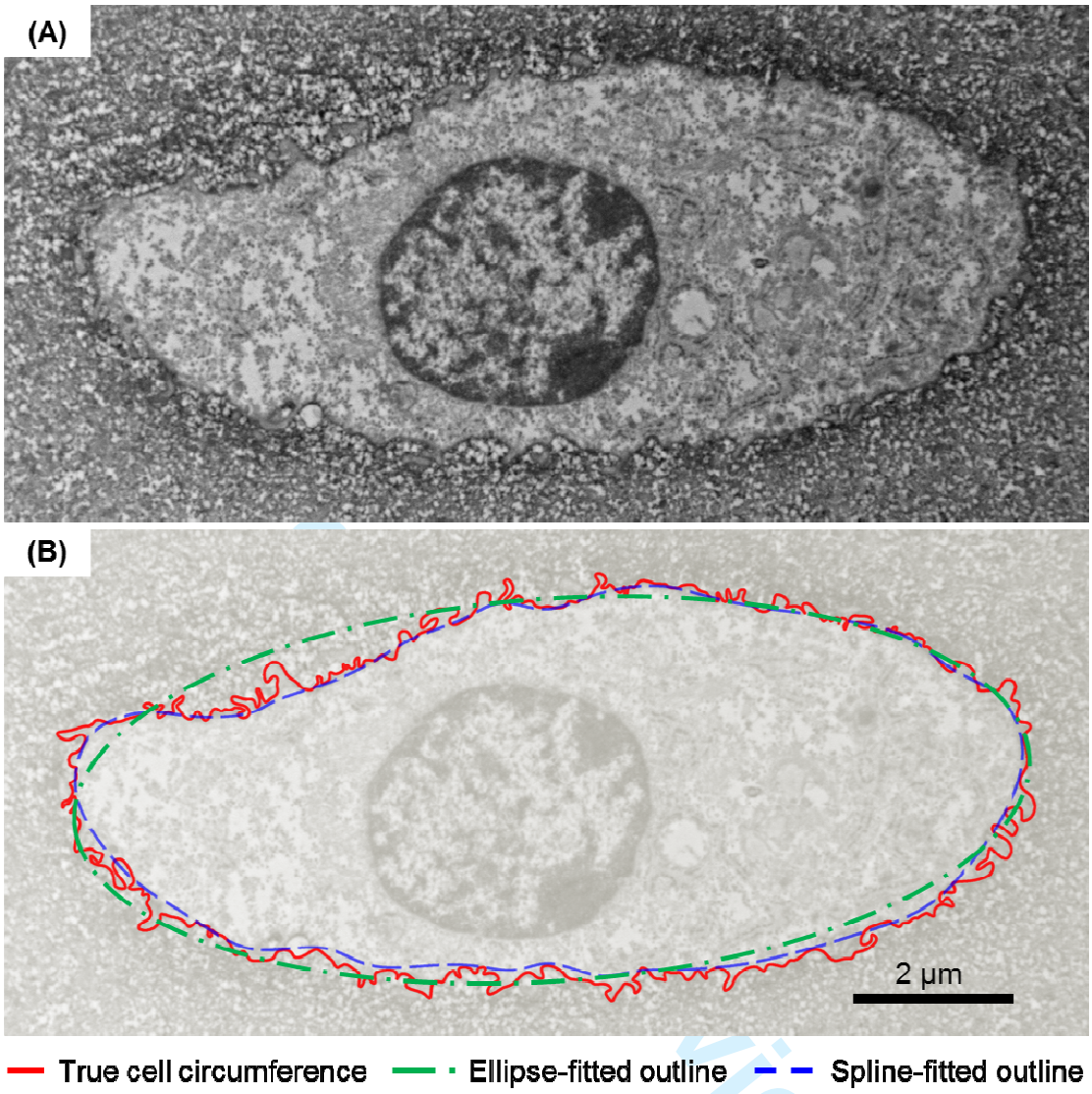

147

148 Fig. 1. Illustration of the steps involved in quantifying the surface roughness. (A) Original
149 electron micrograph of a chondrocyte; (B) same image as in (A), but the image was intentionally
150 brightened in order to highlight the cell circumference. First, the true cell circumference (red
151 solid line) was manually-tracked. The enclosed area was then best-fit to an ellipse (green dashed-
152 dotted line) of equal area and second moment of area. A cubic spline function was also fit to the
153 outline of cells (blue dashed line). The surface roughness was defined as the percentage
154 difference in circumference between the cell and the fitted ellipse (ellipse-fitted roughness) or
155 between the cell and the fitted spline curve (spline-fitted roughness).

156

157 STATISTICAL ANALYSIS

158

159 Data were expressed as means ± 1 standard deviation. The means of the surface roughness and
160 the surface complexity were analysed for loading effect using generalised estimating equations
161 (GEE) to take into account the correlated nature of the observations and the unbalanced study
162 design. Multiple comparisons were accounted for through Holm-Bonferroni adjusted *p*-values.[24]
163 The means of the ellipse-fitted roughness and spline-fitted roughness were compared by paired t-
164 test. Pearson's correlation coefficient was used to investigate the relationship between the
165 membrane surface roughness and the box-counting fractal dimension as well as the relationship
166 between the membrane surface roughness and the cell aspect ratio (α=0.05) (SPSS 20, SPSS Inc.,
167 IL, USA).

For Peer Review

Results

Indentation of cartilage to nominal strains of 50% ($N_{explant}$ = 5), 30% ($N_{explant}$ = 4) and 10% ($N_{explant}$ = 5) resulted in peak stresses of 15.7 ± 1.8 MPa, 5.3 ± 1.1 MPa, and 1.0 ± 0.3 MPa and equilibrium stresses of 1.1 ± 0.1 MPa, 0.4 ± 0.1 MPa and 0.1 ± 0.1 MPa, respectively.

In response to increasing tissue strains, chondrocytes became flatter with their aspect ratio increasing from 2.4 ± 1.1 (0 % strain), to 4.3 ± 1.9 (10% strain), to 6.9 ± 2.2 (30% strain), and to 10.1 ± 3.8 (50% strain).

While the cells became flatter, increasing tissue strains were also associated with a qualitative decrease in membrane surface roughness (Fig. 2). Quantitative analysis confirmed a highly significant decrease in surface roughness (primary y-axis of Fig. 3) with increasing tissue strains ($p<0.0001$, Fig. 3). The decrease in surface roughness was most pronounced upon loading to 10% tissue strains, but continued to decrease for the 30% and 50% tissue strains, albeit to a smaller degree (Fig. 3). A similar trend was also observed for the box-counting dimensional approach as the fractal dimensions of the cell membranes decreased with increasing tissue strains (secondary y-axis of Fig. 3). It should be noted that we observed a high statistical significance ($p < 0.0001$) between the unloaded control group samples and each of the loaded experimental group samples (10% strain, 30% strain and 50% strain). Therefore, only two micrographs from the paired-control samples were randomly selected from each of the loaded samples, and cells used for analysis in the control group samples were obtained from six of the fourteen control explants.

For Peer Review

The relationship between cell shape and membrane ruffles was studied by plotting the ellipse-fitted surface roughness as a function of cell aspect ratio using data that were pooled across all strain conditions. It was found that the ellipse-fitting surface roughness decreased with increasing aspect ratio, with a good logarithmic fit ($r^2 = 0.59$, Fig. 4). In particular, the membrane unfolding seemed to reach a plateau when the cell aspect ratio went beyond 10 (Fig. 4).

There were notable variations in surface roughness of unloaded control cells for specific cell shapes (Fig. 4). Although cells were selected from the top 7.5% of the tissue samples, small differences in the distance from the articular surface to the individual cells may result in a different sensitivity of the membrane strains, and thus the observed variations in surface roughness among the unloaded control cells. However, this is likely not the case because surface roughness was found to be independent of the location in which the chondrocytes reside within this top 7.5% tissue thickness (see Supplementary Materials, S2).

Surface roughness was quantified using cell outlines derived using the best-fitting ellipse and the best-fitting cubic spline approach introduced above. However, there were no differences between results obtained using the ellipse-fitting roughness approach and the spline-fitting roughness approach ($p = 0.353$). In addition, results derived from surface roughness and from surface complexity were also compared. Although using completely different algorithms, the results of membrane surface roughness for the two approaches used here were highly correlated with the results obtained from standard box-counting fractal analysis ($r^2 = 0.78$, Fig. 5).

For Peer Review

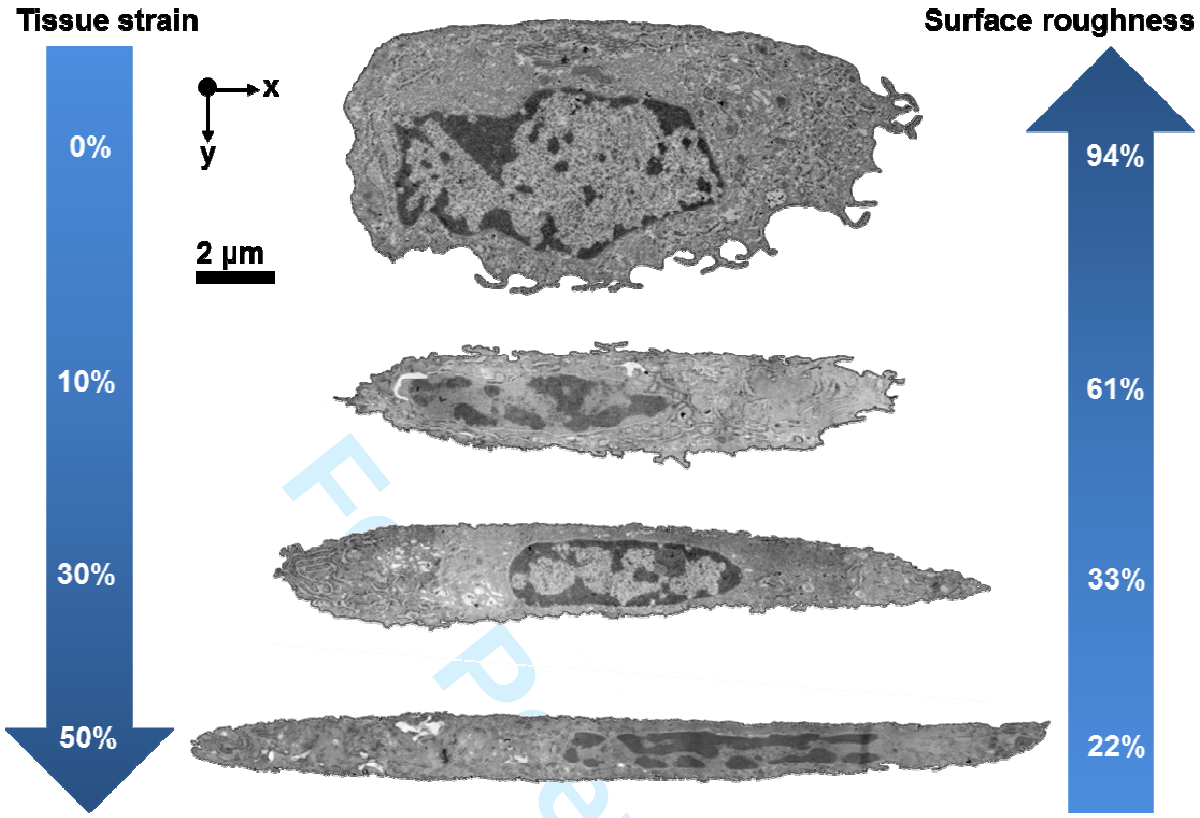

Fig. 2. Representative chondrocyte micrographs from different loading groups showed a decrease in surface roughness with increasing nominal strains applied to the cartilage tissue. The y-axis represents the axis of tissue compression. All analyzed cells resided in the superficial zone of the cartilages (top 7.5% tissue thickness). Scale bar indicates 2µm.

For Peer Review

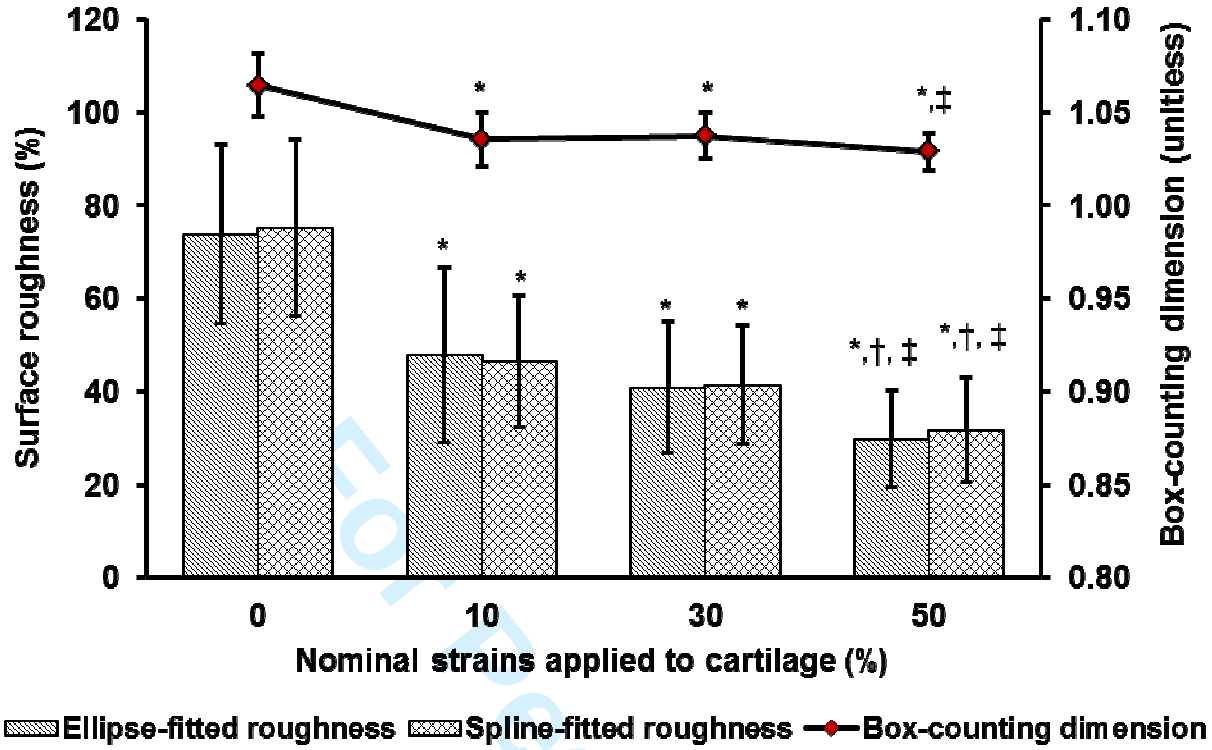

Fig. 3. Membrane surface roughness (primary y-axis) and box-counting fractal dimension (secondary y-axis) of chondrocytes as a function of nominal strains applied to the cartilage (N_{cell} = 22 for each group). The surface roughness and box-counting dimensions decrease as tissue strain increases, suggesting that the chondrocytes unfold their membrane folds during mechanical compression in a load-dependent manner. * indicates significant change in surface roughness and box counting dimensions from unloaded cells ($p<0.0001$). † demonstrates significant difference in surface roughness compared to the group loaded by 10% strain ($p<0.01$). ‡ shows significant difference in surface roughness and box-counting dimension compared to the group loaded by 30% ($p<0.05$).

For Peer Review

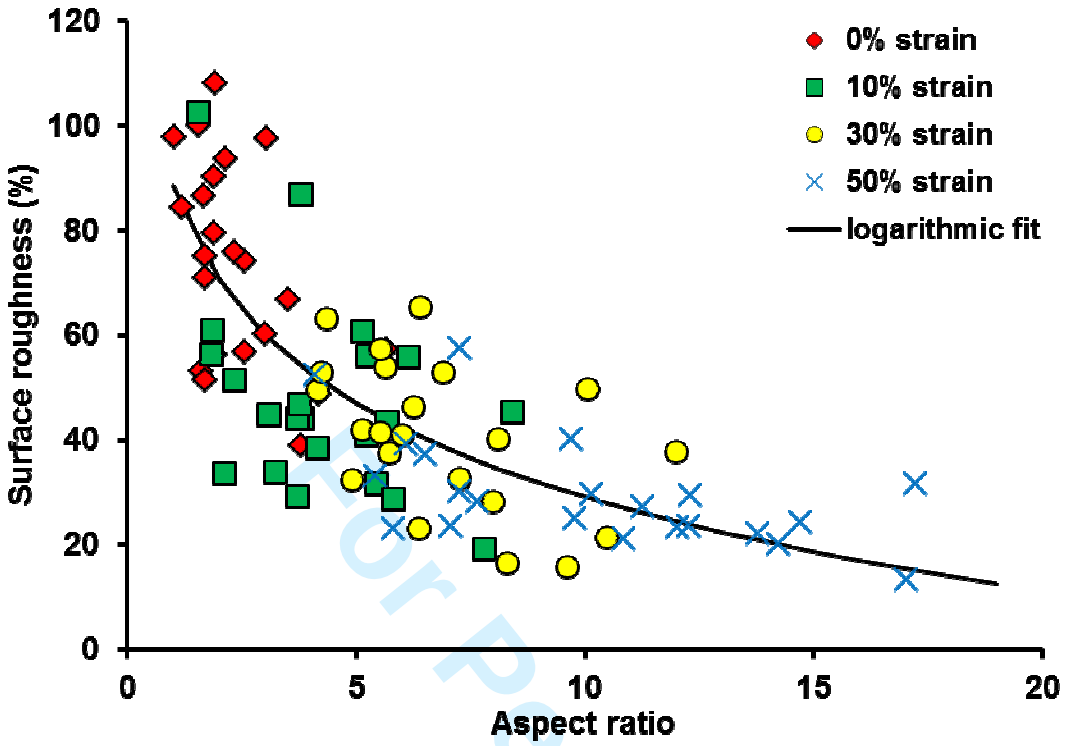

Fig. 4. Scatterplot of the membrane surface roughness from all loading groups (strains of 0 %, 10 %, 30 % and 50 %) as a function of cell aspect ratio (N_{cell} = 22 for each group). As a result of tissue compression, the cell aspect ratio increases (denoting flatter shape). However, the membrane surface roughness decrease with increasing cell aspect ratio, with a good logarithmic fit (r^2=0.59).

For Peer Review

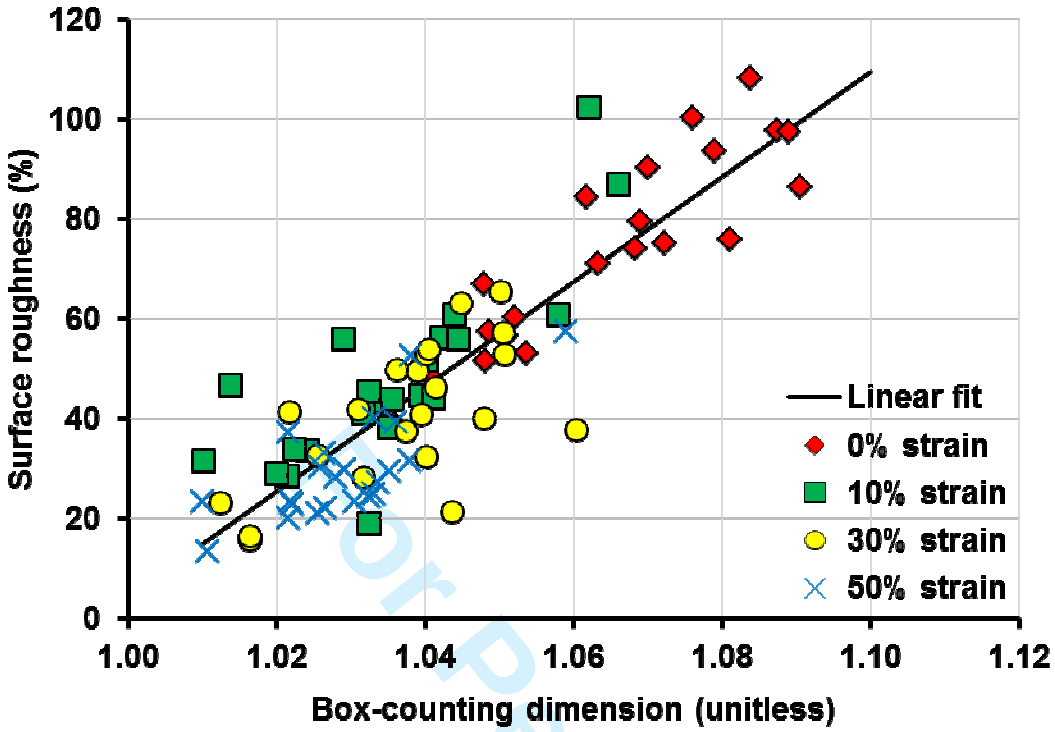

Fig. 5. Relationship between ellipse-fitted membrane surface roughness and box-counting fractal dimensions (N_{cell} = 22 for each group). The standard box-counting approach used for fractal analysis produced results that were highly correlated with the surface roughness defined in the current study (r^2=0.78, $p<0.0001$). The high correlation between the two parameters suggests the soundness of our new definition for 'membrane surface roughness' in quantifying cell surface morphology.

For Peer Review

Discussion

In order to better understand the mechanism of chondrocyte necrosis associated with cartilage impact loading, we previously developed a mechanistic model of impact-induced cell death through theoretical and experimental studies.[11, 18] This model was built on the assumption that cell membranes have waves (ruffles) that unfold when cartilage is compressed. However, such membrane unfolding has neither been shown directly nor has it been quantified. The primary goal of the current study was to establish if chondrocytes unfold their membrane ruffles when exposed to increasing amounts of cartilage compression in their natural extracellular matrix environment, and if so, to quantify the membrane unfolding response. Our results indicate a significant reduction in chondrocyte membrane surface roughness in response to tissue strains, thus providing strong evidence that membrane unfolding is a protective mechanism against membrane rupture (Fig. 2, Fig. 3). Unfolding of the membrane ruffles increased with the magnitude of tissue compression, thereby further supporting our conclusions (Fig. 3, Fig. 4).

Superficial zone chondrocytes were targeted in this study, as impact injuries mostly lead to cell death in superficial zone tissues.[25-27] While the physiological strains of cartilage tissue range from 10-35%,[28, 29] we applied 50% tissue strain to unravel the response of chondrocytes to extreme tissue strains. It should be noted that the compressive strains in the superficial zone tissue are higher than the applied nominal tissue strains due to the lower stiffness of the superficial zone cartilage compared to the mid- and deep zone cartilage.[30] Two completely different methods (membrane surface roughness and membrane fractal dimension) for analyzing cell membrane morphology under compression produced similar results with surprisingly high

For Peer Review

correlations (Fig. 5), thus providing confidence in our definition of 'membrane surface roughness'.

Cell surface ruffles have been regarded for some time as a form of membrane reservoirs[14, 15, 17] that can be used to buffer tensile membrane strains. However, the extent of this potential reservoir and its function in situ have not been quantified. Our results suggest that membrane unfolding occurs to a great extent for small tissue strains (0-10%), with decreasing effect for large strains (10-50%) suggesting that membrane unfolding might protect cells best upon initial tissue loading, and that there may be a limit to the extent of membrane unfolding. Likely, chondrocytes have other protective strategies to keep their membranes intact.

Indeed, the second possible form of protection may come from the caveolar system of chondrocytes. Caveolae are the small flask-shaped invaginations ranging from 60-90 nm diameters in size that lie along the cell membrane.[31, 32] It is thought that the caveolae originate from the incorporation of intracellular lipid vesicles and serve as a form of membrane reservoir that will be used for surface expansion when the cell membrane is under stretch.[33, 34] Previous studies have found that live cells will increase their total membrane surface area when being stretched.[35] Flask shaped caveolae were observed in most of the chondrocytes investigated in this study and a representative image of these in a cell at 30% strain is shown in Figure 6a. Preliminary data on the number of caveolae per cell at each strain are shown in Figure 6b and future studies should investigate this observation more systematically.

For Peer Review

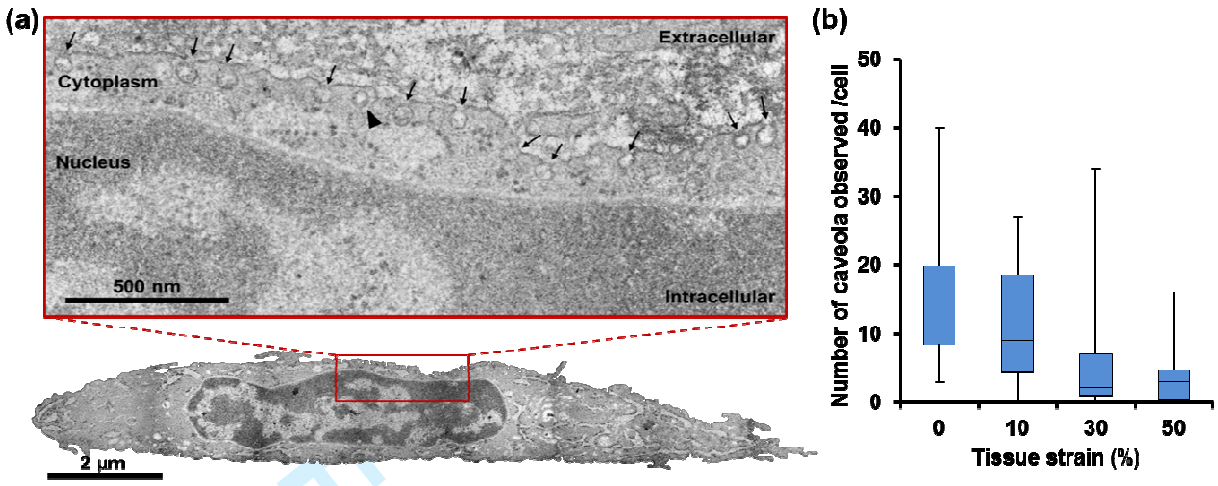

Fig. 6. Caveolae were observed in chondrocytes residing in cartilages that were loaded by 0-50% nominal strain. (a) Characteristic chondrocyte micrograph obtained from cartilage loaded by 30% nominal compressive strain. A local region highlighted by the red square was magnified to show an array of caveolae (small membrane invaginations) lining the plasma membrane. The caveolae either fused with the plasma membrane (arrows) or remained as sub-membrane closed vesicles (arrowhead). Fused caveolae were flask-shaped with an average length of the major axis of 61.5±4.5 nm and minor axis of 48.3±3.2 nm. (b) Box plot of the number of caveolae observed per chondrocyte. There are 22 chondrocytes analyzed in each loading group. The whiskers represent the minimum and maximum number of caveolae observed per cell.

The third possible chondrocyte membrane protective mechanism may be associated with the fluid loss induced by large cell deformation. Cells of identical volumes with a large aspect ratio (flat cells) have a greater surface area than cells with a small aspect ratio (round cells). During cartilage compression, cells become flatter (Fig. 4) and would require up to 3 times the original membrane surface area for the loading conditions used in the current study, if cells were to maintain constant volumes. However, the magnitude of membrane expansion is reduced if cells

For Peer Review

lose volume through fluid loss during tissue loading. Such cell volume losses have been observed for in situ[12, 36] and in vivo[37] chondrocytes under mechanical compression. Therefore, strain-induced volume loss may play a role in reducing membrane strains during cartilage compression.

In addition to providing protection against membrane rupture, the load-induced membrane unfolding may also play an important role in regulating the metabolic behaviour of chondrocytes. The metabolic behaviour of chondrocytes is governed in part by mechanotransduction events at the cell membrane, which are thought to be triggered by local membrane strains.[38, 39] When cell membranes are deformed locally, extracellular mechanical signals may cause intracellular biochemical processes that are activated through 'stretch-activated ion channels' in the cell membrane[40, 41] and/or deformation of the membrane-anchored cytoskeleton.[42] Our results of the membrane unfolding may provide crucial insight into the local deformation of chondrocyte membranes for different tissue loading conditions, and may enhance our understanding of the mechanisms underlying chondrocyte mechanotransduction.

Interestingly, the membrane ruffles in unloaded chondrocytes were asymmetrically distributed (polarity-like). Sections of the membranes facing the articular surface typically showed less ruffles than sections of the membranes facing towards the bone (Fig. 2). Such top-bottom 'polarity' of membrane ruffles may be of functional relevance and may be dictated by the mechanical loading environment experienced by cells, or by the location of specific transmembrane proteins, as has been reported in cell types other than chondrocytes (e.g., epithelial cells).[43] The functional relevance of this asymmetry in membrane ruffles is not known

For Peer Review

and should be studied in the future, as it may contain important information about cell volume regulation and protection of cell membranes against excessive strains. Nevertheless, the results of this study suggest that chondrocyte behaviour and properties should be determined with the cells in their natural in situ state, as cells isolated from their matrix environment lose their in situ shape and asymmetric distribution of membrane ruffles that uniquely characterize the cells under in situ conditions.[21]

This study has limitations that need to be considered when interpreting our results. First, the results presented here represent steady state responses of chondrocytes. Although it is possible that chondrocytes behave differently under dynamic conditions, previous studies found that chondrocytes will reach a 'steady state' shape during continuous dynamic loading.[37, 44] Second, we assumed that the cell membranes unfold instantaneously with cell deformation. However, it is unknown if the membranes unfold in an instantaneous or in a delayed manner when cells undergo shape changes. Due to the limitations of the current technology, the membrane morphology cannot be observed at high resolution in real time. Third, while RHT was used to prevent cell shrinkage from the surrounding ECM,[45] previous studies raised concerns about RHT in inhibiting cell collapse at nominal compressive strains lower than 20%, and in causing vacuole formation in cytosol.[46] However, we found that the mean aspect ratio of the cells increased from 2.4 to 4.3 when the cartilages were loaded by 10% strains, suggesting that the tissue compressive strains were successfully transferred to the cells at low tissue strains. Also, only cells without apparent vacuole in the cytoplasm were used for image analysis. Fourth, live-dead cell assays were not performed in the current study. However, previous studies have shown that chondrocytes remain viable in articular cartilage that is compressed up to 80% nominal strains. [47]

For Peer Review

353 Also, only individual cells with no apparent breach of the plasma membrane were selected for
354 image analysis. Therefore, we are confident that our results represent the response of live cells
355 prior to chemical fixation. Fifth, the varying osmotic conditions in control and experimental
356 tissues due to tissue compaction may result in shrinkage artefacts in chondrocytes exposed to
357 different loading conditions. These artefacts cannot be neglected when comparing cells from
358 different tissue zones (superficial, middle and deep) zones. In order to minimize these artefacts,
359 only cells from the top 7.5% of the tissue thickness were selected for image analysis in the
360 current study. Finally, although this study represents a first step in evaluating the hypothesis of
361 membrane unfolding in live chondrocytes embedded in their natural environment under
362 physiological loading condition, the results of this study are yet to have a clear clinical
363 application.
364
365 In summary, the results of this study led us to the conclusion that chondrocytes unfold their
366 membrane ruffles in a load-dependent manner during physiological loading as a protective
367 measure against cell membrane rupture. However, membrane unfolding is likely not the sole
368 mechanism of membrane protection as chondrocytes may also use the caveolar system and
369 strain-induced volume loss to protect membranes from excessive stretch. These proposed
370 mechanisms need careful investigation in the future.

For Peer Review

Acknowledgments

The authors would like to thank Wei Xiang Dong and Ruth Seerattan for providing technical assistance in histological preparation for electron microscopy, Yasir Al-Saffar for assistance in tissue indentation, Svetlana Kuznetsova for assistance in image analysis, Dr. Tak-Shing Fung for help with statistical analysis, and Dr. Marcelo Epstein for useful discussion on fractal analysis of membrane ruffles.

This study was supported by Alberta Innovates-Health Solutions (AI-HS), the Alberta AI-HS Team grant on osteoarthritis (grant number: 200700596), the NSERC CREATE training program of Biomedical Engineers for the 21st Century (grant number: CREAT/371280-2009), the Canadian Institutes of Health Research (CIHR) (grant number: MOP-111205 and 140824), CIHR Canada Research Chair (grant number: 950-200955) and the Killam Memorial Chair. The aforementioned funding sources had no involvement in the study design, collection, analysis, and interpretation of data, in the writing of the manuscript, and in the decision to submit the manuscript for publication.

Competing interests

No conflicts of interest to report

For Peer Review

References

1. Aigner T, Söder S, Gebhard PM, et al. 2007. Mechanisms of Disease: role of chondrocytes in the pathogenesis of osteoarthritis—structure, chaos and senescence. Nature Reviews Rheumatology 3:391-399.
2. Hashimoto S, Ochs RL, Komiya S, et al. 1998. Linkage of chondrocyte apoptosis and cartilage degradation in human osteoarthritis. Arthritis and Rheumatism 41:1632-1638.
3. Buckwalter JA. 1995. Osteoarthritis and articular cartilage use, disuse, and abuse: experimental studies. J Rheumatol Suppl 43:13-15.
4. Kühn K, D'Lima DD, Hashimoto S, et al. 2004. Cell death in cartilage. Osteoarthritis and Cartilage 12:1-16.
5. Del Carlo M, Jr., Loeser RF. 2008. Cell death in osteoarthritis. Current Rheumatology Reports 10:37-42.
6. Sheetz MP. 2001. Cell control by membrane–cytoskeleton adhesion. Nature Reviews Molecular Cell Biology 2:392-396.
7. Nichol JA, Hutter OF. 1996. Tensile strength and dilatational elasticity of giant sarcolemmal vesicles shed from rabbit muscle. J Physiol 493:187-198.
8. Evans EA, Skalak R. 1979. Mechanics and thermodynamics of biomembranes: part 1. CRC Critical Reviews in Bioengineering 3:181-330.
9. Waugh RE. 1983. Effects of abnormal cytoskeletal structure on erythrocyte membrane mechanical properties. Cell Motility 3:609-622.
10. Nguyen BV, Wang Q, Kuiper NJ, et al. 2009. Strain-dependent viscoelastic behaviour and rupture force of single chondrocytes and chondrons under compression. Biotechnology Letters 31:803-809.
11. Moo EK, Herzog W, Han SK, et al. 2012. Mechanical behaviour of in-situ chondrocytes subjected to different loading rates: a finite element study. Biomechanics and Modeling in Mechanobiology 11:983-993.
12. Moo EK, Han SK, Federico S, et al. 2014. Extracellular matrix integrity affects the mechanical behaviour of in-situ chondrocytes under compression. Journal of Biomechanics 47:1004-1013.
13. Waugh RE, Hochmuth RM. 1987. Mechanical equilibrium of thick, hollow, liquid membrane cylinders. Biophysical Journal 52:391-400.
14. Dai J, Sheetz MP. 1998. Cell Membrane mechanics. Methods in cell biology: Academic Press; pp. 157-171.
15. Raucher D, Sheetz MP. 1999. Characteristics of a membrane reservoir buffering membrane tension. Biophysical Journal 77:1992-2002.
16. Petty HR, Hafeman G, McConnell HM. 1981. Disappearance of Macrophage Surface Folds after Antibody-Dependent Phagocytosis. The Journal of Cell Biology 89:223-229.
17. Li Z, Anvari B, Takashima M, et al. 2002. Membrane tether formation from outer hair cells with optical tweezers. Biophysical Journal 82:1386-1395.
18. Moo EK, Amrein M, Epstein M, et al. 2013. The Properties of Chondrocyte Membrane Reservoirs and Their Role in Impact-Induced Cell Death. Biophysical Journal 105:1590-1600.

For Peer Review

19. Vlahakis NE, Schroeder MA, Pagano RE, et al. 2002. Role of Deformation-induced Lipid Trafficking in the Prevention of Plasma Membrane Stress Failure. Am J Respir Crit Care Med 166:1282-1289.
20. Dai J, Sheetz MP, Wan X, et al. 1998. Membrane tension in swelling and shrinking molluscan neurons. The Journal of Neuroscience: The Official Journal of the Society for Neuroscience 18:6681-6692.
21. Guilak F, Erickson GR, Ting-Beall HP. 2002. The Effects of Osmotic Stress on the Viscoelastic and Physical Properties of Articular Chondrocytes. Biophysical Journal 82:720-727.
22. Lee DA, Knight MM, F. Bolton J, et al. 2000. Chondrocyte deformation within compressed agarose constructs at the cellular and sub-cellular levels. Journal of Biomechanics 33:81-95.
23. Mulchrone KF, Choudhury KR. 2004. Fitting an ellipse to an arbitrary shape: implications for strain analysis. Journal of Structural Geology 26:143-153.
24. Bender R, Lange S. 2001. Adjusting for multiple testing—when and how? Journal of Clinical Epidemiology 54:343-349.
25. Bourne DA, Moo EK, Herzog W. 2015. Cartilage and chondrocyte response to extreme muscular loading and impact loading: Can in vivo pre-load decrease impact-induced cell death? Clinical Biomechanics 30:537-545.
26. Lewis JL, Deloria LB, Oyen-Tiesma M, et al. 2003. Cell death after cartilage impact occurs around matrix cracks. Journal of Orthopaedic Research 21:881-887.
27. Krueger JA, Thisse P, Ewers BJ, et al. 2003. The extent and distribution of cell death and matrix damage in impacted chondral explants varies with the presence of underlying bone. Journal of Biomechanical Engineering 125:114-119.
28. Guterl CC, Gardner TR, Rajan V, et al. 2009. Two-dimensional strain fields on the cross-section of the human patellofemoral joint under physiological loading. Journal of Biomechanics 42:1275-1281.
29. Wan L, de Asla RJ, Rubash HE, et al. 2008. In vivo cartilage contact deformation of human ankle joints under full body weight. Journal of Orthopaedic Research: Official Publication of the Orthopaedic Research Society 26:1081-1089.
30. Schinagl RM, Gurskis D, Chen AC, et al. 1997. Depth-dependent confined compression modulus of full-thickness bovine articular cartilage. Journal of Orthopaedic Research: Official Publication of the Orthopaedic Research Society 15:499-506.
31. Wilsman NJ, Farnum CE, Reed-Aksamit DK. 1981. Caveolar system of the articular chondroycte. Journal of Ultrastructure Research 74:1-10.
32. Yamada E. 1955. The fine structure of the gall bladder epithelium of the mouse. J Biophys Biochem Cytol 1:445-458.
33. Sinha B, Köster D, Ruez R, et al. 2011. Cells Respond to Mechanical Stress by Rapid Disassembly of Caveolae. Cell 144:402-413.
34. Kozera L, White E, Calaghan S. 2009. Caveolae Act as Membrane Reserves Which Limit Mechanosensitive ICl,swell Channel Activation during Swelling in the Rat Ventricular Myocyte. PLoS ONE 4.
35. Fisher JL, Levitan I, Margulies SS. 2004. Plasma Membrane Surface Increases with Tonic Stretch of Alveolar Epithelial Cells. Am J Respir Cell Mol Biol 31:200-208.

For Peer Review

36. Guilak F, Ratcliffe A, Mow VC. 1995. Chondrocyte deformation and local tissue strain in articular cartilage: a confocal microscopy study. Journal of Orthopaedic Research 13:410-421.
37. Abusara Z, Seerattan R, Leumann A, et al. 2011. A novel method for determining articular cartilage chondrocyte mechanics in vivo. Journal of Biomechanics 44:930-934.
38. Leong DJ, Hardin JA, Cobelli NJ, et al. 2011. Mechanotransduction and cartilage integrity. Annals of the New York Academy of Sciences 1240:32-37.
39. Sachs F. 2010. Stretch-Activated Ion Channels: What Are They? Physiology 25:50-56.
40. Sachs F. 1991. Mechanical transduction by membrane ion channels: a mini review. Mol Cell Biochem 104:57-60.
41. Mobasheri A, Lewis R, Maxwell JEJ, et al. 2010. Characterization of a stretch-activated potassium channel in chondrocytes. Journal of Cellular Physiology 223:511-518.
42. Ingber D. 1991. Integrins as mechanochemical transducers. Current Opinion in Cell Biology 3:841-848.
43. St Johnston D, Ahringer J. 2010. Cell Polarity in Eggs and Epithelia: Parallels and Diversity. Cell 141:757-774.
44. Han S-K, Madden R, Abusara Z, et al. 2012. In situ chondrocyte viscoelasticity. Journal of Biomechanics 45:2450-2456.
45. Hunziker EB, Herrmann W, Schenk RK. 1982. Improved cartilage fixation by ruthenium hexammine trichloride (RHT): A prerequisite for morphometry in growth cartilage. Journal of Ultrastructure Research 81:1-12.
46. Szafranski JD, Grodzinsky AJ, Burger E, et al. 2004. Chondrocyte mechanotransduction: effects of compression on deformation of intracellular organelles and relevance to cellular biosynthesis. Osteoarthritis and Cartilage 12:937-946.
47. Madden R, Han SK, Herzog W. 2012. Chondrocyte deformation under extreme tissue strain in two regions of the rabbit knee joint. Journal of Biomechanics.

For Peer Review

Figure legends

Fig. 1. Illustration of the steps involved in quantifying the surface roughness. (A) Original electron micrograph of a chondrocyte; (B) same image as in (A), but the image was intentionally brightened in order to highlight the cell circumference. First, the true cell circumference (red solid line) was manually-tracked. The enclosed area was then best-fit to an ellipse (green dashed-dotted line) of equal area and second moment of area. A cubic spline function was also fit to the outline of cells (blue dashed line). The surface roughness was defined as the percentage difference in circumference between the cell and the fitted ellipse (ellipse-fitted roughness) or between the cell and the fitted spline curve (spline-fitted roughness).

Fig. 2. Representative chondrocyte micrographs from different loading groups showed a decrease in surface roughness with increasing nominal strains applied to the cartilage tissue. The y-axis represents the axis of tissue compression. All analyzed cells resided in the superficial zone of the cartilages (top 7.5% tissue thickness). Scale bar indicates 2μm.

Fig. 3. Membrane surface roughness (primary y-axis) and box-counting fractal dimension (secondary y-axis) of chondrocytes as a function of nominal strains applied to the cartilage (N_{cell} = 22 for each group). The surface roughness and box-counting dimensions decrease as tissue strain increases, suggesting that the chondrocytes unfold their membrane folds during mechanical compression in a load-dependent manner. * indicates significant change in surface roughness and box counting dimensions from unloaded cells ($p<0.0001$). † demonstrates significant difference in surface roughness compared to the group loaded by 10% strain ($p<0.01$).

For Peer Review

‡ shows significant difference in surface roughness and box-counting dimension compared to the group loaded by 30% ($p<0.05$).

Fig. 4. Scatterplot of the membrane surface roughness from all loading groups (strains of 0 %, 10 %, 30 % and 50 %) as a function of cell aspect ratio (N_{cell} = 22 for each group). As a result of tissue compression, the cell aspect ratio increases (denoting flatter shape). However, the membrane surface roughness decrease with increasing cell aspect ratio, with a good logarithmic fit (r^2=0.59).

Fig. 5. Relationship between ellipse-fitted membrane surface roughness and box-counting fractal dimensions (N_{cell} = 22 for each group). The standard box-counting approach used for fractal analysis produced results that were highly correlated with the surface roughness defined in the current study (r^2=0.78, $p<0.0001$). The high correlation between the two parameters suggests the soundness of our new definition for 'membrane surface roughness' in quantifying cell surface morphology.

Fig. 6. Caveolae were observed in chondrocytes residing in cartilages that were loaded by 0-50% nominal strain. (a) Characteristic chondrocyte micrograph obtained from cartilage loaded by 30% nominal compressive strain. A local region highlighted by the red square was magnified to show an array of caveolae (small membrane invaginations) lining the plasma membrane. The caveolae either fused with the plasma membrane (arrows) or remained as sub-membrane closed vesicles (arrowhead). Fused caveolae were flask-shaped with an average length of the major axis of 61.5±4.5 nm and minor axis of 48.3±3.2 nm. (b) Box plot of the number of caveolae observed

For Peer Review

per chondrocyte. There are 22 chondrocytes analyzed in each loading group. The whiskers represent the minimum and maximum number of caveolae observed per cell.

For Peer Review